Christian Hirt · Jakob Flury

Astronomical-topographic levelling using high-precision astrogeodetic vertical deflections and digital terrain model data

Abstract At the beginning of the 21st century, a technological change took place in geodetic astronomy by the development of Digital Zenith Camera Systems (DZCS). Such instruments provide vertical deflection data at an angular accuracy level of $0\rlap{.}''1$ and better. Recently, DZCS have been employed for the astrogeodetic collection of dense sets of vertical deflection data in several test areas in Germany with high-resolution digital terrain model (DTM) data $(10-50\,\mathrm{m}$ resolution) avail-

C. Hirt

Institut für Erdmessung, Universität Hannover, Germany. Now at: Department of Geomatics, HafenCity University Hamburg, Hebebrandstr. 1, 22297 Hamburg, Germany

E-mail: Chris.Hirt@web.de Tel.: +49 42827 5323

J. Flury

Institut für Astronomische und Physikalische Geodäsie, Technische Universität München, Germany. Now at: Center for Space Research, 3925 W Braker Lane #200, Austin, Texas 78759, USA

E-mail: jflury@csr.utexas.edu Tel.: +1 512 232 1987

able. These considerable advancements motivate a new analysis of the method of astronomical-topographic levelling, which uses DTM data for the interpolation between the astrogeodetic stations. We present and analyse a least-squares collocation technique that uses DTM data for the accurate interpolation of vertical deflection data. The combination of both data sets allows a precise determination of the gravity field along profiles, even in regions with a rugged topography. The accuracy of the method is studied with particular attention on the density of astrogeodetic stations. The error propagation rule of astronomical levelling is empirically derived. It accounts for the signal omission that increases with the station spacing. In a test area located in the German Alps, the method was successfully applied to the determination of a quasigeoid profile of 23 km length. For a station spacing from a few 100 m to about 2 km, the accuracy of the quasigeoid was found to be about $1-2$ mm, which corresponds to a relative accuracy of about $0.05-0.1$ ppm. Application examples are given, such as the local and regional validation of gravity field models computed from gravimetric data and the economic gravity field determination in geodetically less covered regions.

1 Introduction

The method of astronomical levelling provides quasigeoid or geoid differences between two or more stations by the integration of vertical deflections along a connecting path (e.g., Torge 2001; Bomford 1980). Vertical deflections are obtained by means of astrogeodetic observations at stations where the geodetic co-

ordinates are known. Introduced by Helmert (1884), astronomical levelling was applied for gravity field determination at local and regional scales over several decades – from Galle (1914) in the Harz Mountains in Germany to the European geoid by Levallois and Monge (1978) – until gravimetric methods evolved and became a standard. In many regions, large gravity data sets became available and enabled a precise gravimetric gravity field determination, applying Stokes's formula (e.g., Torge 2001).

Precise astronomical levelling basically requires a dense set of vertical deflections with sufficient spatial resolution along a profile, so that the shape of the gravity field is represented properly and the deflection data may be interpolated reliably. In the past, the determination of vertical deflections in a dense arrangement by means of astrogeodetic techniques was costly and time-consuming. Therefore, vertical deflections were often only available at widely spaced stations (e.g. $10 - 50$ km).

In many cases, linearly interpolated vertical deflections between distant astrogeodetic stations do not sufficiently represent the actual gravity field, particularly not in mountainous regions (e.g., Bosch and Wolf 1974). In order to keep the interpolation error between adjacent stations small – despite a large spacing – the theory of astronomical levelling has been extended to astrogravimetric levelling and astronomical-topographic levelling. *Astrogravimetric levelling* utilises gravimetric measurements for the interpolation of vertical deflections (e.g., Molodenski *et al.* 1962, Campbell 1971).

The method of *astronomical-topographic levelling* uses topographic reductions of vertical deflections for the interpolation between astrogeodetic stations. It

accounts for the fact that in mountainous areas a large part of the vertical deflection signal is caused by topographic masses (e.g., Forsberg and Tscherning 1981). Helmert (1901) already pointed out that a simple and smoothed behaviour of vertical deflections may be expected by removing the gravitational attraction of the topography from the observations, aiming at a more reliable interpolation. First studies on the computation of topographic vertical deflections, necessary for such topographic reductions, were performed by Niethammer (1932), Meier (1956) and Kobold (1957) for Switzerland's classical astronomical levelling profiles. The topographic reductions were computed from local terrain data decomposed into radial-symmetric sectors.

The use of topographic deflections, computed from gridded digital terrain model (DTM) data for reducing observed vertical deflections, was investigated by Heitz (1968) for the gravity field determination in Germany and by Elmiger (1969) for Switzerland. Elmiger used polynomials for the interpolation of the smoothed data, whereas Heitz applied the more sophisticated interpolation approach of least-squares collocation (LSC). In sequence, several studies on the use of topographic data for smoothing and prediction of vertical deflections were published, e.g. by Bosch and Wolf (1974), Boedecker (1976), Gurtner (1978), Forsberg and Tscherning (1981), Moritz (1983), Bürki (1989) and Marti (1997).

In these publications, the spacing between observed vertical deflection stations is mostly on the order of 10 km (or even more). Furthermore, the vertical deflection data available for the listed studies was determined partly by visual observations with classical astrogeodetic instruments (e.g. Kern DKM3A, astrolabe), and partly with photographic (analogue) zenith cameras, developed between $1970 - 1980$.

The accuracy of the vertical deflection data was generally assumed to be about $0''\!.3 - 0''\!.5$ (cf. Heitz 1968, Elmiger 1969, Bürki 1989, Marti 1997).

In recent years, a significant technological change took place in geodetic astronomy by the development of Digital Zenith Camera Systems (DZCS) in Hanover and Zurich (e.g. Bürki *et al.* 2004, Hirt 2004, Hirt and Bürki 2002). These new measurement systems provide vertical deflections accurate to $0''\!.08 - 0''\!.1$ (e.g., Hirt and Seeber 2005, Hirt *et al.* 2006), requiring relatively short observation and processing times of a total of about 20 min per station. These significant improvements with respect to the analogue era of geodetic astronomy recently led to an extended application of DZCS for astrogeodetic gravity field studies. New astrogeodetic data sets became available with a high spatial resolution (50 m to several 100 m) in several test areas in Northern Germany and Bavaria (e.g. Hirt 2004, Hirt and Seeber 2005, Hirt *et al.* 2006).

Considering the research on astronomical-topographic levelling carried out in the last century, there are three essential reasons for a reconsideration of how to combine astronomical deflections with DTM data. The first reason is the significant improvement of the accuracy of the DZCS vertical deflection data by a factor of five. The second reason refers to the much higher spatial resolution of the new vertical deflection data sets (about two orders of magnitude). The third reason is related to the increased accuracy and spatial resolution of present DTM data sets, provided e.g. by national or state survey authorities (e.g., $10 - 50$ m resolution) or available from the Shuttle Radar Topography Mission (SRTM, 90 m resolution).

The objective of this work on astronomical-topographic levelling is the economical combination of the new high-precision astrogeodetic DZCS vertical de-

flection data sets and DTM data on a local scale, allowing us to determine the gravity field along lines and profiles at an accuracy level of about 0.1 ppm (1 mm over 10 km) and better. The combination approach conceptually follows the one proposed by Heitz (1968). The test area used in this study is an alpine valley (elevation $800 - 1000$ m), located in the Bavarian Alps. The available vertical deflection data set of about 100 stations has already been successfully used for the validation of different gravimetric gravity field models (cf. Hirt *et al.* 2006).

This paper is organised as follows: Sect. 2 briefly reviews the theory of astronomical levelling. The test area, the astrogeodetic data set and DTMs used for this study are described in Sect. 3. The computation of topographic vertical deflections from the DTM data is treated in Sect. 4. The combination of observed and computed deflections by a remove-restore technique and the interpolation using LSC is dealt with in Sect. 5. The results of the astrogeodetic quasigeoid computation are given in Sect. 6. An accuracy analysis is presented in Sect. 7, with particular focus on the density of astrogeodetic stations required to attain a certain level of accuracy. Concluding remarks and some application examples for the high-precision astronomical-topographic levelling approach are given in Sect. 8.

2 Theory of astronomical levelling

The relatively simple theory of astronomical levelling is described, e.g., in Helmert (1884, 1901), Heiskanen and Moritz (1967), Bomford (1980) and Torge (2001). The method requires observations of astronomical latitude Φ and longi-

tude Λ as well as the geodetic (ellipsoidal) coordinates latitude φ and longitude λ at a number of stations along the path. Vertical deflections

$$\xi = \Phi - \varphi \tag{1}$$

$$\eta = (\Lambda - \lambda) \cos \varphi \tag{2}$$

are the measure for the inclination of the equipotential surface with respect to the ellipsoid at the Earth's surface. They are also known as surface vertical deflections or Helmert deflections (e.g., Torge 2001, Jekeli 1999).

The integration of vertical deflections (ξ, η) along the path gives the difference of the geoid undulation

$$\Delta N_{AB} = - \int_A^B \varepsilon ds - E_{AB}^O \tag{3}$$

or quasigeoid undulation

$$\Delta \zeta_{AB} = - \int_A^B \varepsilon ds - E_{AB}^N, \tag{4}$$

respectively, between stations A and B.

$$\varepsilon = \xi \cos \alpha + \eta \sin \alpha \tag{5}$$

is the vertical deflection component along the azimuth α, and ds refers to the station spacing. The product εds expresses the height difference of the equipotential surface between the adjacent stations. Evaluating the integral in Eqs. (3) and (4) presupposes a dense coverage of vertical deflections so that the interpolation between adjacent stations i and $i + 1$ may be done linearly:

$$\varepsilon = \frac{\varepsilon_i + \varepsilon_{i+1}}{2}. \tag{6}$$

The orthometric correction E_{AB}^O accounts for the curvature of the plumbline, reducing the integrated deflections to the geoid. Analogously, the normal correc-

tion E_{AB}^N is applied in order to compute the quasigeoid undulations between A and B (Heiskanen and Moritz 1967, Torge 2001):

$$E_{AB}^O = \int_A^B \frac{g - \gamma_0^{45}}{\gamma_0^{45}} dn + \frac{\overline{g}_A - \gamma_0^{45}}{\gamma_0^{45}} H_A - \frac{\overline{g}_B - \gamma_0^{45}}{\gamma_0^{45}} H_B,$$

(7)

$$E_{AB}^N = \int_A^B \frac{g - \gamma_0^{45}}{\gamma_0^{45}} dn + \frac{\overline{\gamma}_A - \gamma_0^{45}}{\gamma_0^{45}} H_A - \frac{\overline{\gamma}_B - \gamma_0^{45}}{\gamma_0^{45}} H_B.$$

(8)

The computation of the normal correction E_{AB}^N requires the knowledge of the surface gravity g along the profile, which may be obtained from gravity databases. The height differences dn between adjacent stations as well as the heights above mean sea level (MSL) of the first station H_A and last station H_B and may be easily derived from DTM data. Comparisons between computations of the normal correction E_{AB}^N from heights derived from different DTM data sets (Sect. 3.3) showed an influence below 0.1 mm in our test area. Therefore, heights taken from the DTM data are accurate enough for the computation of E_{AB}^N.

For the mean normal gravities $\overline{\gamma}_A, \overline{\gamma}_B$ at the profile's first and last station, the vertical gradient and the normal gravity is computed using the rigorous formulae of the normal gravity field (cf. Torge 2001, p. 106 and 112). γ_0^{45} is an arbitrary constant value, but usually the normal gravity at latitude $\varphi = 45°$ is used. The computation of the orthometric correction E_{AB}^O, as opposed to the normal correction E_{AB}^N, requires density hypotheses in order to obtain the mean gravity $\overline{g}_A, \overline{g}_B$ along the plumbline (cf. Torge 2001, p. 82, Tenzer *et al.* 2005).

The computations performed in this work are restricted to the normal correction, and thus refer to the quasigeoid domain. Hirt *et al.* (2006) showed that for the Bavarian test area, the normal correction E_{AB}^N may be computed accurate to

$0.1 - 0.15$ mm. These numbers mainly reflect the errors of surface gravity predicted from gravity databases (about 1 mgal prediction accuracy in our case). As a consequence, in areas with good gravity data coverage the accuracy of the normal correction is insignificant to the error budget of astronomical-topographic levelling (Sect. 7). The corrections E_{AB}^0 and E_{AB}^N are not treated further in this study.

3 Test area and data sets

3.1 Test area

The Technical University of Munich established a gravity field research test area with an extent of about 20 km by 20 km in the Estergebirge mountains in the Alps south of Munich. Since 1994, a large number of precise observations of various gravity field quantities (such as gravity, geometric levelling and GPS height measurements) were carried out. The project aims at a precise analysis and modelling of the contribution of mountain topography to the gravity field and at the investigation of consequences for geodetic purposes (Flury 2002).

A large and dense gravity data set was used to study short-wavelength signal characteristics (Flury 2006). Precision levelling is available up to the summits and was used to study height accuracies and differences between various height system definitions (Flury 2002). Along the levelling lines, numerous GPS/levelling stations allow a comparison with quasi/geoid models (Flury *et al.* 2006). Astronomical coordinates were observed for 35 stations with various techniques at an accuracy level of about $0''\!.5$ before the new astrogeodetic measurement campaign in 2005.

3.2 Astrogeodetic vertical deflections

The TZK2-D DZCS, developed at the University of Hanover from $2001 - 2003$, is the sensor used in this study. This new astrogeodetic observation system was applied for the collection of vertical deflection data at 103 new stations. The stations are along a profile oriented in a near North-South direction (Fig. 1). The profile length is about 23.3 km and the average station spacing is approximately 230 m.

The collection of the vertical deflection data was completed during a total observation period of four weeks in the northern autumn 2005. The observed data sets were processed using the Hanover astrogeodetic processing software AURIGA (Hirt 2004). The celestial reference was provided by the new high-precision UCAC (U.S. Naval Observatory CCD Astrograph Catalogue, Zacharias *et al.* 2004) and Tycho-2 (Høg *et al.* 2000) star catalogues. The campaign and processing statistics are given in Table 1.

Table 1 near here

During the campaign, 38 stations were observed twice on different nights. The standard deviation obtained from the residuals is found to be $0''\!.082$ both for ξ and η. This accuracy estimate agrees well with values from other astrogeodetic measurement campaigns with the same instrument (cf. Hirt and Seeber 2005, Hirt 2006). The distribution of the TZK2-D stations and the acquired (ξ, η) data is shown in Fig. 1 in the context of the local topography.

Fig. 1 near here

3.3 Digital Terrain Model data

For the area around the profile, two high resolution DTM grids from the Bayerisches Landesamt für Vermessung und Geoinformation (LVG, Bavarian State Geodetic Survey) were used, a new 10 m grid (about 1 m vertical accuracy) and a 12 year old 50 m grid ($2 - 3$ m vertical accuracy). Both height grids were compared at identical grid points. Differences were found to be below ± 10 m in most cases, with a mean value of 0.27 m and a root mean square (RMS) of 2.8 m. These values indicate a good quality of both models.

The southernmost part of the profile is at 1 km distance from the border between Germany and Austria, where the high resolution LVG DTM grids end. Beyond this area, the USGS global $30''$ DTM data set *gtopo30* was used. A 600 m westward shift of the gtopo30 DTM data was detected and corrected for. For further studies, the *gtopo30* model may be replaced by the global DTM of the GLOBE (NOAA Global Land One-kilometer Base Elevation Digital Elevation Model) project, which has the same grid resolution and seems to have a slightly better quality in our area. The global SRTM DTM has not been used so far as it has gaps in our test area.

4 Computation of topographic deflections from DTM data

Topographic deflections $(\xi, \eta)_{top}$ are the contributions of topographic masses (above the geoid) to the surface vertical deflections. They are determined from DTM data. For an accurate combination with astrogeodetic deflections (Sect. 5) it is important to select a sufficient DTM grid resolution, a sufficient DTM extent and a representation of the DTM grid elements by adequate bodies.

In particular, the short-scale components of the topographic deflections, originating from the innermost zone around each computation point, must be computed as accurately as possible (e.g., Marti 1997). With increasing distance from the computation point, the DTM resolution can be reduced and the accuracy requirements can be relaxed.

Table near here

Table 2 shows the grid resolution of the used DTM grids for each distance zone. According to Marti (1997), errors of the total topographic deflection should be well below $0''\!.1$ with the selected grid mesh widths. A representation of each grid mesh by a right rectangular prism (cuboid) was used. The horizontal components of the attraction of a cuboid are obtained by (Mader 1951, Tsoulis 1999, Nagy *et al.* 2000, 2002, Tsoulis 2001)

$$V_x = G\rho \left|\left|\left| y\operatorname{arsinh}\frac{z}{\sqrt{x^2+y^2}} + z\operatorname{arsinh}\frac{y}{\sqrt{x^2+z^2}} - \right.\right.\right.$$

$$\left.\left.\left. -x\arctan\frac{yz}{x\sqrt{x^2+y^2+z^2}}\right|_{x_1}^{x_2}\right|_{y_1}^{y_2}\right|_{z_1}^{z_2}$$

(9)

$$V_y = G\rho \left|\left|\left| z\operatorname{arsinh}\frac{x}{\sqrt{y^2+z^2}} + x\operatorname{arsinh}\frac{z}{\sqrt{x^2+y^2}} - \right.\right.\right.$$

$$\left.\left.\left. -y\arctan\frac{xz}{y\sqrt{x^2+y^2+z^2}}\right|_{x_1}^{x_2}\right|_{y_1}^{y_2}\right|_{z_1}^{z_2}$$

with the gravitational constant G, topographic mass-density ρ, and the coordinates with respect to the computation point x_i, y_i, z_i of the prism faces (Nagy *et al.* 2000).

A standard rock density of 2670 kg/m^3 was used. Differences between this standard value and the true rock density are taken into account by the observed surface vertical deflections in the remove-restore procedure, cf. Sect. 5. The total

topographic attractions $(V_x, V_y)^{top}$ are obtained by summation over all grid elements. From the horizontal components of topographic attraction, topographic deflections

$$\xi_{top} = \frac{V_y^{top}}{\gamma} \qquad \text{and} \qquad \eta_{top} = \frac{V_x^{top}}{\gamma} \qquad (10)$$

are obtained. For the normal gravity γ, a mean value of the area is sufficient.

The $(\xi, \eta)_{top}$ contribution of innermost zone 1 (Table 2) was computed using a 10 m and 50 m DTM resolution. The statistics of the differences are given in Table 3. The RMS of about $0''.02$ is well below the errors of astrogeodetic observations (about $0''.08$), while the extrema can be significant with respect to the astrogeodetic accuracy. Hence, for the combination with astrogeodetic deflections a 50 m grid in general is sufficient, but a 10 m grid can lead to improvements in some cases (see Fig. 2).

As a third alternative, the zone 1 contributions have been computed using polyhedra (Petrović 1996, Tsoulis 2001). In this approach, the innermost zone terrain surface is represented by inclined triangles. The triangular mesh grid includes the computation point itself (cf. Tsoulis 2001). This provides, in general, a better approximation of reality, compared to flat cuboid tops. Table 3 gives the statistics of differences of a polyhedra solution with respect to the 10 m cuboid solution. The RMS is smaller than that of the differences between 50 m and 10 m cuboids. Only in a few cases, the differences still exceed the astrogeodetic observation accuracy. Thus, when no 10 m grid is available, a polyhedra representation based on a 50 m grid can provide very good results (cf. Fig. 2).

Fig. 2 near here

Somewhat larger differences are obtained when grids from the older and newer LVG DTM models are used (cf. Sect. 3.3) which typically differ by only a few metres. The statistics are also given in Table 3. This indicates that a DTM with an accuracy of a few metres should be used for precise astronomical-topographic levelling.

Table 3 near here

In the area crossed by the astrogeodetic profile, some considerable density anomalies of up to 700 kg/m^3 exist, such as low-density quaternary valley sediments. Information on density and geometry of such anomalous bodies is available from refraction seismics, geo-electric observations and gravimetry (Flury 2002). Models of these bodies could be integrated in the remove-restore procedure.

This was not done here since our astronomical observations are densely spaced enough to recover the effects of density anomalies well. If, however, larger distances between observation stations are used, density anomalies can introduce considerable interpolation errors, cf. Sect. 7. Also, the long-wavelength gravity field structures are well recovered by the astrogeodetic observation data, therefore no reduction of an isostatic compensation model or a global gravity field model was applied.

A dense set of 1021 topographic deflections $(\xi, \eta)_{top}$ was computed comprising the 103 observation sites and nine intermediate stations for each profile section between adjacent observation sites. Thereby a dense station spacing of about 23 m was obtained. The geodetic coordinates (φ, λ) of the intermediate stations were linearly interpolated between the observation sites. The corresponding heights H

above MSL were interpolated from the DTM in order to obtain a profile integration path which follows the actual topographic surface as close as possible.

5 Combination of astrogeodetic and topographic deflections by LSC

The aim of *astronomical-topographic levelling* is to obtain very densely sampled, quasi-continuous surface vertical deflections between the astrogedeodetic stations. This requires interpolation, which should be carried out without significant loss of accuracy. A classical remove-restore approach is applied: Topographic deflections (from Sect. 4) are removed from the astrogeodetic vertical deflection observations. The smooth residual signal is interpolated in intermediate stations. Finally, topographic deflections are restored in these intermediate stations in exactly the same way used for the remove step, leading to a dense set of surface vertical deflections.

5.1 Removal of the topography

The input data used for the combination is the set of 103 stations with astrogeodetic vertical deflections $(\xi, \eta)_{obs}$ and the set of 1021 topographic deflections $(\xi, \eta)_{top}$. Both data sets are shown in Fig. 3 (a) as a function of the profile distance. The observed $(\xi, \eta)_{obs}$ and topographic deflections $(\xi, \eta)_{top}$ are strongly correlated. This shows the sensitivity of vertical deflections to the attraction of the topographic masses.

Figure 3 (b) demonstrates that the topographic reduction of the astrogeodetic deflections $(\xi, \eta)_{obs}$ – in the manner "observed - computed" – leads to a much smoother data set

$$(\Delta\xi, \Delta\eta) = (\xi, \eta)_{obs} - (\xi, \eta)_{top}. \tag{11}$$

The same $(\Delta\xi, \Delta\eta)$ data is also depicted in Fig. 3 (c), however at a larger vertical scale for a better view of the details. The apparent features may be subdivided into three categories:

1. Systematic offsets, in particular in the $\Delta\xi$ component (about $10''$), may result from isostatic compensation, from topographic masses beyond the DTM area considered, and from any other long-wavelength features that have not been reduced from the observation data.

2. Wave-like structures, which appear in the $(\Delta\xi, \Delta\eta)$ data, can be attributed to density anomalies in the local topography with respect to the density of the topography introduced in Eq. (9). The presence of such signals with wavelengths of a few kilometres underlines the importance of sufficiently dense observations of vertical deflections for astronomical-topographic levelling. Comparable to gravity anomalies, reduced vertical deflections $(\Delta\xi, \Delta\eta)$ carry essential information of residual gravity field features. From the geophysical point of view, these wave-like structures provide interesting information on the density distribution. They may be used for a check or a refinement of density models.

3. High-frequency structures may reflect very small-scale density anomalies, random errors of the astrogeodetic observations and uncertainties attributable to the DTM data. A further reason for the appearance of small peak-like structures may be a change in azimuth of the profile. This is seen in Fig. 3 (c), for component $\Delta\xi$, at km $2-4$, and for component $\Delta\eta$, at km $14-17$. Here, the profile sections change direction (cf. Fig. 1). In Sect. 5.2.3, the role of these peaks is discussed further.

5.2 Interpolation using LSC

The smooth $(\Delta\xi, \Delta\eta)$ data set is suited for the interpolation applying the standard technique of LSC and prediction (cf. Moritz 1980). The general form of the LSC observation equation reads:

$$\mathbf{l} = \mathbf{Ax} + \mathbf{s} + \mathbf{n} \tag{12}$$

where $\mathbf{l}$ is the vector containing the reduced vertical deflection set $\Delta\xi$

$$\mathbf{l}^T = [\Delta\xi_1, \Delta\xi_2, ..., \Delta\xi_{103}] \tag{13}$$

and for $\Delta\eta$,

$$\mathbf{l}^T = [\Delta\eta_1, \Delta\eta_2, ..., \Delta\eta_{103}], \tag{14}$$

respectively.

Both deflection components are processed separately. The parameter vector $\mathbf{x}$ consists of the corresponding profile distances ranging from 0 km to about 23 km. The product $\mathbf{Ax}$ expresses the deterministic part, and $\mathbf{s}$ is the signal vector containing the correlated wave-like structures. The uncorrelated astronomical observation errors as well as errors from the DTM are represented by the noise vector $\mathbf{n}$. The stochastic properties are described by the signal covariance matrix $\mathbf{C}$ and the noise covariance matrix $\mathbf{D}$. For the noise covariance matrix $\mathbf{D}$, uncorrelated noise of $0''\!.1$ is introduced for the a priori standard deviation σ_n, accounting for random errors of the astrogeodetic observations and DTM data.

5.2.1 Covariance function

Fig. 4 near here

For the design of the signal covariance matrix $\mathbf{C}$, information on the autocorrelation between adjacent stations is used, which is provided by the covariance function $\mathrm{cov}(\mathbf{l}, \mathbf{l}')$. The empirical autocorrelation function computed from the $\Delta\xi$ and $\Delta\eta$ data series is shown in Fig. 4. Due to the relative small number of deflections, seen from the statistical point of view, the empirical functions are considered to provide rather vague information on the correlation. The correlation length (the lag with correlation ρ of 0.5) is found to be 1600 m for $\Delta\xi$ and 2400 m for $\Delta\eta$, respectively.

An exponential model was introduced as the analytical covariance function

$$cov(\mathbf{l}, \mathbf{l}') = \sigma_s^2 \exp^{-0.5a\,\mathrm{dist}(\mathbf{l},\mathbf{l}')} \tag{15}$$

where σ_s is the a priori standard deviation of the signal, set to $0''\!.5$, and a is the correlation length. Other analytical covariance functions (e.g., linear or Gaussian) as well as different correlation lengths were tested. They showed however just a minor influence on the LSC results.

The described LSC approach decomposes the $(\Delta\xi, \Delta\eta)$ deflection data into the filtered component

$$\mathbf{l}_{fil} = \mathbf{A}\mathbf{x} + \mathbf{s} \tag{16}$$

and the residual noise vector $\mathbf{n}$

$$\mathbf{n} = \mathbf{l} - \mathbf{l}_{fil}, \tag{17}$$

which is depicted in Fig. 3 (d). For the subset of 918 intermediate stations, the LSC method provides predicted values $(\Delta\xi, \Delta\eta)_{prd}$, which are shown in Fig. 3 (c).

5.2.2 RMS computed from the noise vector

The noise vector contains the errors from the astrogeodetic observations, the DTM data and model errors (e.g., peaks due to azimuth changes). The RMS values of the $(\Delta\xi, \Delta\eta)$ deflection data, as obtained from the noise vector, are listed in Table 4 with respect to the three different DTM data sets used for the computation of the topographic deflections. They are found to be on the $0\rlap{.}{''}08 - 0\rlap{.}{''}09$ level.

Table 4 near here

This very low noise is an independent confirmation of the estimated accuracy of observation of $0\rlap{.}{''}082$ obtained from repeated observations (Sect. 3.2). Moreover, these accuracy numbers indicate that the three DTM data sets are almost equally suited for the reduction of topographic deflections and that the contribution of errors due to the applied reduction is small.

5.2.3 Changes in azimuth of the profile

The LSC treats the reduced deflections $\Delta\xi$ and $\Delta\eta$ separately in a one-dimensional way as a function of the profile distance. This is mathematically correct if all profile stations are arranged in a straight line. Unfortunately, this condition cannot be strictly met in most cases, particularly not in mountainous areas. Changes in the azimuth of the profile may lead to noise-like peaks in the deflection data, as mentioned in Sect. 5.1 and visible in Fig. 5.

In a rigorous approach, the reduced deflections $\Delta\xi$ and $\Delta\eta$ must be treated in two dimensions, as functions both of latitude φ and longitude λ, e.g., by using a two-dimensional LSC approach. This would, however, require a more areal coverage of the input data and may therefore not work in our case.

Another solution is to introduce a smaller correlation length in Eq. (15) so that the peaks are not filtered in the LSC process. A comparison of test data sets, computed from different correlation lengths ranging from 500 m to 1600 m showed an influence of the quasigeoid computation of a few 0.1 mm. Therefore, the problem of the misalignment of the stations with respect to a straight line plays a minor role in this study.

5.3 Restoration of topography

Finally, the topographic effect $(\xi, \eta)_{top}$ is restored both at the observed stations and at the predicted intermediate stations so that a dense data set of predicted (surface) deflections

$$(\xi, \eta)_{prd} = (\Delta\xi, \Delta\eta)_{prd} + (\xi, \eta)_{top}, \tag{18}$$

is obtained with a sampling about every 23 m (Fig. 3 e). A detailed view of the interpolated surface deflections is given in Fig. 5, which shows a smooth behaviour of the predicted data at very short scales.

Fig. 5 near here

When only a 46 m sampling is used instead of the full 23 m sampling, signal features of at most $0''1$ amplitude are missed, typically at places where the profile runs across breaklines of the topography. We conclude that the chosen 23 m sampling is dense enough to represent the variability of surface deflections along our profile, even in sections with rough topography. This quasi-continuous representation allows a rigorous evaluation of the path integral of Eqs. (4) to (6) along the path on the actual surface of topography.

6 The astrogeodetic quasigeoid profile

The 103 astrogeodetic vertical deflections $(\xi, \eta)_{obs}$, were combined with the topographic deflections $(\xi, \eta)_{top}$, following the procedure described in Sect. 5. The resulting 1021 predicted deflections $(\xi, \eta)_{prd}$ were then integrated along the path, as described in Sect. 2, and the normal correction (Eq. 8) was added (cf. Hirt *et al.* 2006). The astrogeodetic quasigeoid profile is shown in Fig. 6.

Fig. 6 near here

A strong trend in southern direction of about 1.3 m over a distance of 23 km is visible, reflecting the gravitational attraction of the masses of the central Alps. The fine structure of the astrogeodetic profile – a wave-like feature – becomes visible by a simple trend reduction (bottom part of Fig. 6). Here again, small sharp peaks result from azimuth changes discussed above and must not be interpreted as fine structure of the gravity field.

7 Accuracy analysis

7.1 Remarks on the methodology

Before analysing the accuracy of astronomical-topographic levelling in more detail, the general methodology is introduced. The station density and, hence, the *spacing between the astrogeodetic stations* is considered to be the most important parameter in astronomical-topographic levelling. Due to the improved accuracy of astronomical observations, this applies in our case for very short distances (several 100 m).

For an economical application to gravity field determination, it is necessary to know the minimum number of astrogeodetic stations for attaining a certain level of accuracy over a given profile length. Therefore, it is crucial to analyse the accuracy of the gravity field prediction between adjacent stations as a function of the station spacing and, in particular, the prediction of local structures using DTM data.

It is a fortunate situation to have a high-resolution vertical deflection data set with 103 stations on a profile length of about 23 km for this analysis. This data set consists of many more stations than typically required for reliable astrogeodetic modelling of the local gravity field. Therefore, the data set is well-suited to be decomposed into various subsets, consisting of e.g. 10 or 20 stations, in order to simulate various station densities.

By comparing the quasigeoid profiles computed from the subsets with the reference solution, it is possible to study the attainable accuracy as a function of the station spacing. The reference solution denotes the astrogeodetic quasigeoid computed from the full deflection data set (103 observed stations). The comparison between the subsets and the reference solution provides empirical accuracy estimates for predicted vertical deflections and for the gravity field determination.

The prediction accuracy may be easily quantified by comparing the predicted values $(\xi, \eta)_{prd}$ against the corresponding values $(\xi, \eta)_{obs}$, which were not used for the prediction. The prediction error $(\delta\xi, \delta\eta)$ then reads:

$$\delta\xi = \xi_{obs} - \xi_{prd} \tag{19}$$

$$\delta\eta = \eta_{obs} - \eta_{prd}. \tag{20}$$

The set of $(\delta\xi, \delta\eta)$ differences may be used for the computation of statistical quantities, e.g., RMS values. This analysis method is applied in Sect. 7.2.

The second method (Sect. 7.3) is the comparison of astrogeodetic quasigeoid profiles computed from different subsets of observed vertical deflections. Such a solution is stored in a vector

$$\mathbf{\Delta}\zeta = [\Delta\zeta_2, \Delta\zeta_3, ..., \Delta\zeta_n], \tag{21}$$

which contains the quasigeoid heights for the profile stations $2...n$ with respect to the first station. Differences $\delta\mathbf{\Delta}\zeta$ of the profiles may be computed either by comparing a subset solution $\mathbf{\Delta}\zeta^{subset}$ with a reference solution $\mathbf{\Delta}\zeta^{ref}$

$$\delta\mathbf{\Delta}\zeta = \mathbf{\Delta}\zeta^{subset} - \mathbf{\Delta}\zeta^{ref} \tag{22}$$

or with respect to another, independent subset:

$$\delta\mathbf{\Delta}\zeta = \mathbf{\Delta}\zeta^{subset1} - \mathbf{\Delta}\zeta^{subset2}. \tag{23}$$

Differences $\delta\mathbf{\Delta}\zeta$ of the profiles are characterised by their minimal, maximum and mean values, as well as by the RMS. Despite the fact that the subsets and the reference solution are not disjoint, reasonable accuracy estimates are obtained. This is because reference solutions computed from those stations *not* contained in the subset are almost identical with the reference solution computed from the full data set of 103 stations.

Formation of subsets In order to analyse the role of the station spacing in astronomical-topographic levelling, subsets are formed in such a way that only every second, third or fourth station of the full data set is considered. Thereby station densities of 460 m, 690 m, and 920 m, respectively, are simulated. In order to increase the statistical reliability of the results, for each spacing class, subsets are formed by an additional shift of one or more stations before averaging the resulting statistics. The formation of the subsets is demonstrated in Table 5. The

maximum station spacing is about 8 km, corresponding to about one third of the total profile length.

Table 5 near here

Example Figure 7 (a) shows the 21 astrogeodetic vertical deflections ξ_{obs} the subset 5_0 (Table 5) consists of. Following the combination approach described in Sect. 5, the observations are reduced with the set of topographic deflections ξ_{top} (Fig. 7 b). Vertical deflections at intermediate points are predicted (Fig. 7 b), and eventually the topographic effect is restored (Fig. 7 c).

In turn, the complete data set of predicted deflections $(\xi, \eta)_{prd}$ may be used for a quasigeoid computation to be compared with the reference solution (Eq. 22). In addition, the prediction results ξ_{prd} may be compared with the astrogeodetic ξ_{obs} values (Fig. 7 d, Eqs. 19 and 20) in order to assess the accuracy of the prediction.

Fig. 7 near here

7.2 Prediction accuracy

The first analysis focuses on the accuracy of predicted vertical deflections $(\xi, \eta)_{prd}$. All subsets without shifts (subsets 2_0 to 35_0, cf. Table 5) were used for the prediction of deflections, applying the remove-restore procedure. The results were compared against those astrogeodetic observations not used for the prediction, serving as independent information. T

The statistics computed from the differences (Eqs. 19 and 20) are given in Table 6 for selected spacing classes up to 8050 m. The RMS prediction error for subsets 2_0 to 35_0 is shown in Fig. 8. The RMS values include astrogeodetic

observation errors (Sect. 3.2) and small errors due to changes of the azimuth of the profile (Sect. 5.2.3), but mainly the omission error discussed below.

Table 6 near here

Fig. 8 near here

It is seen that a station spacing up to 1 km allows us to predict deflections at the $0\rlap{.}''2$ accuracy level. For distances up to 2 km, the prediction accuracy is $0\rlap{.}''3 - 0\rlap{.}''5$. A further enlargement of the spacing to about $5 - 8$ km significantly degrades the accuracy up to about $3''$, although the contribution of the topography was rigorously taken into account by the remove-restore procedure.

The decrease of the prediction accuracy reflects the *omission* of the fine structure of the gravity field. Fine signals as seen in Fig. 7 (b) – which are related to density anomalies not considered in the remove-restore procedure – are not sufficiently sampled by a spacing of several kilometres. For such spacings, prediction using topographic deflections $(\xi, \eta)_{top}$ does not allow any more a full reconstruction of the gravity field between observed deflections $(\xi, \eta)_{obs}$.

For spacings beyond 4 km, the omission error for ξ is larger than for η, which is because some major density anomalies are in the east-west direction across the profile. The omission error does not only depend on the sampling of the signal, but also on local signal variability. In mountains, the signal variability tends to be larger than in flat terrain, even if the contribution of topography has been removed, cf. Flury (2006). Consequently, a smaller omission error can be expected for profiles in flat terrain.

The RMS values of $0\rlap{.}''11$ and $0\rlap{.}''12$ for ξ and η obtained for subset 2_0 with the shortest spacing reflect the errors of the observed deflections, of azimuthal

changes (Sect. 5.2.3) and already contain a small omission error. These values are in good agreement with the accuracy of the observations discussed in Sects. 3.2 and 5.2.

7.3 Accuracy of the quasigeoid profiles

7.3.1 Accuracy assessment for the reference profile

Due to the dense station spacing of 460 m, the subsets 2_0 and 2_1 are appropriate to estimate the accuracy of the reference quasigeoid profile in good approximation. As both subsets are disjoint, they may be used for the computation of two independent quasigeoid profiles. The difference between the two profiles $\delta \Delta \zeta$ (Eq. 23) is depicted in Fig. 9 and the related statistics are given in Table 7.

Fig. 9 near here

Table 7 near here

The maximum difference between both profiles is about 1.5 mm and the RMS computed from the differences is about 0.9 mm. The RMS value accounts for the statistical uncertainties contained in both independent data sets. Therefore, the related standard deviation of the single profiles is assumed to improve with $\sqrt{2}$ to the level of 0.6 mm. These numbers demonstrate that the accuracy of astronomical-topographic levelling is at the millimetre level and better for a station spacing of a few 100 m and for the profile length of 23 km.

7.3.2 Remove-restore procedure compared with simple linear interpolation

The following comparison shows the significant accuracy advantage of the described remove-restore LSC technique over an interpolation of surface deflections

without DTM data, as used in simple astronomical levelling. Applying the LSC technique with topographic reductions, 35 different astrogeodetic quasigeoid profiles were computed for the spacing classes 230 m to 8050 m (reference profile and subsets 2_0 to 35_0). The procedure was repeated, using a simple linear interpolation between the observed deflections without any topographic information. These two sets of quasigeoid profiles were compared to the reference profile (Eq. 22).

Table 8 lists the maximum differences as well as the RMS for both techniques as a function of the station spacing. For most of the spacing classes, the comparison reveals an accuracy advantage of LSC with DTM data over the linear interpolation by about one order of magnitude. Already reaching 1 mm for the 230 m resolution, the RMS deteriorates to about $1 - 2$ cm for a spacing of about 1 km when the topography is neglected. A spacing of several kilometres further degrades the accuracy of simple astronomical levelling to the decimetre level. The error of astronomical-topographic levelling is found to be at the millimetre level, though also increasing with station spacing due to the increasing omission error, cf. Sect. 7.2.

Table 8 near here

7.3.3 Role of different DTM data

The role of the DTM resolution for astronomical-topographic levelling was studied as follows. The complete range of the observed deflection subsets (Table 5) was combined with the topographic deflections $(\xi, \eta)_{top}$ computed from a variable innermost zone (50 m cuboids, 50 m polyhedra and 10 m cuboids), but constant outer zones (cf. Table 2). For each of the three topographic deflection data sets,

630 different quasigeoid profiles were computed from subsets 2_0 to 35_34 as well as from the full deflection data set.

The RMS values were computed from the differences $\delta\Delta\zeta$ of the profiles, obtained by the comparison with the reference profile (Eq. 22). Eventually, the RMS values for each spacing class were averaged, separately for the three DTM data sets. Figure 10 shows that the three curves coincide almost perfectly. The differences between the curves are on the order of 0.2 mm. Hence, in practice the RMS values for a given spacing are independent of the DTM data used.

Figure 10 near here

A detailed result of this comparison is given in Fig. 11. It shows the comparison of the three quasigeoid profiles, which were computed from the three topographic data sets and the full $(\xi, \eta)_{obs}$ data set. The differences are about $0.1-0.2$ mm, as such insignificant.

Fig. 11 near here

The approach used for the computation of topographic deflections $(\xi, \eta)_{top}$ (cuboids or polyhedra) plays a minor role when the high-resolution 50 m DTM data is used. Besides, no significant differences were found between the results obtained from 50 m DTM data and 10 m DTM data. These results implicitly include the influence of the different vertical accuracies of the DTM data. Moreover, it was shown in Sect. 4 that the vertical accuracy of the DTM has an influence on topographic deflections similar to that of the differences between the variants of DTM resolution.

The general conclusion is that the a DTM with a spatial resolution of about 50 m and related vertical accuracy of about $2-3$ m is completely sufficient for

high-precision astronomical-topographic levelling. With respect to the current accuracy level of the astrogeodetic data, a higher spatial resolution of the DTM data does not significantly increase the method's accuracy.

7.4 Error propagation of astronomical-topographic levelling

In Sects. 7.2 and 7.3, it was shown how the errors of astronomical-topographic levelling due to the gravity field omission error increase with the spacing between the observation stations. As the astrogeodetic quasigeoid is determined by integration over the profile path (cf. Eq. 4), the quasigeoid errors accumulate along the path (visible in Fig. 9), in analogy to the error propagation in geometric levelling. Thus, the accuracy of a quasigeoid difference between two points depends on the observation station spacing and the overall distance between the two points. The statistical results presented in Sect. 7.3 refer to the specific profile length of 23 km.

It is useful to derive a more universal empirical rule for the error propagation in astronomical-topographic levelling. Such a rule should provide information on the relative accuracy attainable over arbitrary profile lengths, e.g. 10 km or 100 km, as a function of the station spacing. A transformation of the accumulated RMS values from the given 23 km profile length to precise accuracy estimates for arbitrary profile lengths seems to be rather difficult.

Therefore, the 629 astrogeodetic quasigeoid profiles computed from the subset range 2_0, 2_1, ... 35_33, 35_34 were analysed in the following way: Within each of the quasigeoid profiles, all possible profile sections with a length of approximately

10 km were extracted and compared against the corresponding profile sections of the reference profile, yielding residual errors

$$\varepsilon_{\Delta\zeta} = \Delta\zeta_j^{subset} - \Delta\zeta_j^{ref} - (\Delta\zeta_i^{subset} - \Delta\zeta_i^{ref}) \tag{24}$$

where the indices i and j refer to those station pairs with a spacing of 10 km.

The set of residuals $\varepsilon_{\Delta\zeta}$ obtained from each of these comparisons were used for the computation of the formal standard deviation:

$$\sigma = \sqrt{\frac{1}{n}\sum_1^n \varepsilon_{\Delta\zeta}^2} \tag{25}$$

with n total number of extracted profile sections. Finally, the results of each spacing class (460 m: two values, 690 m: three values of the standard deviation, etc.) were averaged in order to increase the statistical reliability.

The computed standard deviation σ for the profile length of 10 km is shown as function of the station spacing in Fig. 12. The method of astronomical-topographic levelling may provide astrogeodetic quasigeoid profiles at an accuracy level of about 0.5 mm, when the spacing of the astrogeodetic stations is about $500-700$ m. This estimation is in good agreement with the assessment given Sect. 7.3 (0.6 mm over 23 km). Up to a station spacing of about 1 km, the accuracy is found to be better than 1 mm. With such a spacing, the astrogeodetic quasigeoid profiles still contain almost the full gravity field signal.

Fig. 12 near here

A slight loss of accuracy occurs for station spacings between 1.5 km and 2 km, where an accuracy level of $1-2$ mm over 10 km distance is attained. Consequently, the very fine structure of the gravity field is not completely reconstructed by the combination with DTM data. For station spacings increasing from 2 km to about 8 km, the accuracy degrades – in good approximation – linearly to about 15 mm,

reflecting the increasing omission error. Obviously a significant part of the fine structure of the real gravity field is not recovered any more by such large station spacings.

Applying the general propagation law of variances, the standard deviations for each station spacing may now be scaled to other profile lengths l, e.g. 100 km, by multiplying with the factor

$$f = \sqrt{\frac{l\text{[km]}}{10\text{[km]}}}. \tag{26}$$

Some accuracy estimates, interpolated from the standard deviations shown in Fig. 12, are listed in Table 9, as well as the scaled values for different profile lengths, ranging from 10 km to 400 km. The impact of omitted gravity field structures due to the station spacing is covered by the given values. Table 9 allows us to estimate the accuracy of quasigeoid height differences $\Delta\zeta$ determined with astronomical-topographic levelling. For example, a profile length of about 60 km length may be determined at the 1 cm accuracy level when the spacing of the astrogeodetic stations is 3 km.

Table 9 near here

Table 9 shows the advantages and drawbacks of astronomical-topographic levelling. It can provide quasigeoid accuracies at the millimetre level over short distances with a limited number of observations. Over several hundred kilometres, an accuracy better than the centimetre level is still achievable. However, due to accumulation of errors, this would require not only a considerable expense in terms of observations (station spacings of 2 km or less), but also a detailed analysis of remaining systematic errors possibly contained in the data.

It should be noted that the results here implicitly refer to an accuracy level of observed deflection data $(\xi, \eta)_{obs}$ of $0.''08 - 0.''1$. Therefore, the practical use of Table 9, e.g., for planning other gravity field studies, presupposes astrogeodetic data of comparable accuracy as well as DTM data with a similar resolution and vertical accuracy. On the other hand, it should be recalled that our results refer to astronomical-topographic levelling in mountains where the gravity field variability tends to be higher. In flat terrain, in general somewhat better accuracies can be expected.

Role of systematic errors As the method of astronomical levelling is based on integration, even small systematic errors quickly degrade the attainable accuracy. The UCAC star catalogue is known to contain systematic position errors of about $0.''01$, whereas the Tycho-2 catalogue is considered to be practically free of systematic error sources (Zacharias *et al.* 2000). In order to control the processing of the DZCS observations, both the UCAC and the Tycho-2 catalogue were applied.

A second reason for using UCAC is related to the fact that Tycho-2 did not provide enough reference stars for the processing of all astrogeodetic observations. The definitive vertical deflection data $(\xi, \eta)_{obs}$ used in this study was computed as the average of the solutions obtained from both catalogues. Hence it is reasonable to assume a remaining systematic error $\Delta\varepsilon$ of about $0.''005$.

As a rule of thumb, a systematic error of $1''$ causes an offset $\Delta_{\Delta\zeta}$ in the computed quasigeoid of 5 mm over a profile length of 1 km (= 5 ppm). Hence, the propagation of systematic errors $\Delta\varepsilon$ over arbitrary profile distances d is estimated as follows:

$$\Delta_{\Delta\zeta} = 5 \, \text{mm} \frac{\Delta\varepsilon}{1''} \frac{d[\text{km}]}{1[\text{km}]}. \tag{27}$$

The systematic error $\Delta\varepsilon$ of about $0\rlap{.}{''}005$, attributable to the star catalogue, is therefore estimated to cause an quasigeoid offset $\Delta_{\Delta\zeta}$ of 0.25 mm and 2.5 mm over distances of 10 km and 100 km, respectively. A comparison with the accuracy numbers given in Table 9 shows that systematic errors play an important role in the error budget of astronomical-topographic levelling with station spacings from a few 100 m to about 2 km.

Another known error source with systematic behaviour is the effect of anomalous refraction, which may affect the astrogeodetic observations. The characteristics of anomalous refraction (e.g., amplitudes and fluctuation) were studied in the time-domain at one selected station outside the working area (cf. Hirt 2006). This study found that anomalous refraction usually may reach amplitudes from $0\rlap{.}{''}05$ up to about $0\rlap{.}{''}2$ at frequencies of some hours.

The spatial behaviour (e.g., correlation of astrogeodetic observations at adjacent stations), however, is still unknown and cannot be quantified. As the astrogeodetic data used for this study was acquired in different weather situations during an observation period of four weeks, and at stations with heterogeneous environmental conditions, it seams reasonable to assume that systematic errors due to anomalous refraction plays no significant role for this study. This assumption is corroborated by the differences obtained from 38 repeated observations performed in different nights (Sect. 3.2), which show no significant systematics and follow a normal distribution.

8 Conclusions and applications

The method of astronomical-topographic levelling was investigated with focus on the combination of high-precision astrogeodetic with topographic vertical deflections computed from DTM data. The attainable accuracy of local quasigeoid profiles was analysed. The use of topographic data for the interpolation of astrogeodetic vertical deflections keeps the interpolation error small and thus reduces the number of astrogeodetic measurements needed.

The general conclusion of this study is that astronomical-topographic levelling provides information on the geometry of the local gravity field (e.g., quasigeoid or equipotential surfaces) at an accuracy level of $0.05 - 0.1$ ppm when the astrogeodetic stations are densely arranged (several 100 m up to 2 km). For station spacings of $3 - 6$ km and profile lengths of several 10 km, the accuracy of quasigeoid profiles is around $0.2 - 0.5$ ppm. Due to the Alpine environment of the test area (e.g., surrounding rugged topography and mass-density variations) the results are assumed to be representative – at least not too optimistic – for most other areas.

Depending on the application and desired accuracy, the derived error propagation rule of astronomical levelling may assist in deciding on the appropriate station spacing. For station spacings from a few 100 m to about 1 km, gaps between the astrogeodetic stations are almost adequately bridged by the topographic deflections. For a larger station spacing of several kilometres however, the signal omission error rules the attainable accuracy level, as the gravity field's fine structure is not completely accounted for. Small systematic error sources are found to dominate the error budget only when the astrogeodetic stations are densely spaced.

The remarkable accuracy of astronomical-topographic levelling is attributed both to the unprecedented accuracy of the astrogeodetic observations of about $0''.08 - 0''.01$, and to the improved efficiency achieved by DZCS, as well as to the high-resolution DTM data sets used in the combination.

The use of different DTM sets with spatial resolutions of 10 m and 50 m and vertical accuracies of about $1 - 3$ m revealed no significant impact on the results. Therefore a DTM resolution of about 50 m and a vertical accuracy of about 3 m is considered to be sufficient for astronomical-topographic levelling. The investigation of astronomical-topographic levelling using DTM data with somewhat lower spatial resolution, such as the 90 m SRTM data, remains as a future task.

Applications Due to its very low noise level, the technique of astronomical-topographic levelling is well-suited for the local and regional validation of gravity field models derived from other observables, e.g., gravity, GPS/levelling or satellite data. Such a validation project is currently ongoing in Germany from the Harz mountains to the Bavarian Alps (cf. GOCE GRAND 2005). The local validation of gravimetric gravity field models and GPS/levelling by means of astrogeodetic-topographic levelling was already performed with success by Hirt *et al.* (2006) and Flury *et al.* (2006).

A further interesting application field is the calibration and validation of INS/GPS vector gravimetric measurement systems. Currently, minor use is being made of the vertical deflections as obtained by those systems (Jekeli and Li 2006). A dense set of precise predicted vertical deflections, provided by astronomical-topographic levelling, may help to obtain a proper accuracy assessment of INS/GPS systems for 3D-vector gravimetry.

Another possible application is the efficient local gravity field determination along profiles in geodetically less developed regions, e.g., for hydraulic engineering projects in South America or Africa. Here, the decided advantage of the astronomical-topographic levelling technique is that, apart from the DTM data, no gravity field observations are required outside the working area – other than in the gravimetric method.

For example, a quasigeoid profile of 100 km length is assumed to consist of 50 astrogeodetic stations. Using a DZCS, the required vertical deflection data may be observed in $3 - 5$ clear nights. The combination with topographic deflections, computed e.g. from available SRTM terrain data, is expected to provide an accuracy of the quasigeoid on the centimetre level. Hence, astronomical-topographic levelling may be an economic and accurate technique for gravity field surveys in such areas.

References

Boedecker G (1976). *Astrogravimetrisch-topographisches Nivellement*. Wiss. Arb. Lehrst. für Geod., Phot. und Kart. Techn. Univ. Hannover Nr. 64

Bomford G (1980). *Geodesy, Fourth Edition*. Clarendon Press, Oxford

Bosch W, Wolf H (1974). *Über die Wirkung von topographischen Lokal-Effekten bei profilweisen Lotabweichungs-Prädiktionen.* Mitteilungen aus dem Institut für Theoretische Geodäsie der Universität Bonn Nr. 28

Bürki B (1989). *Integrale Schwerefeldbestimmung in der Ivrea-Zone und deren geophysikalische Interpretation.* Geodätisch-geophysikalische Arbeiten in der Schweiz, Nr. 40. Schweizerische Geodätische Kommission

Bürki B, Müller A, Kahle H-G (2004). *DIADEM: The New Digital Astronomical Deflection Measuring System for High-precision Measurements of Deflections of the Vertical at ETH Zurich.* Electronic Proc. IAG GGSM2004 Meeting in Porto, Portugal. Published also in: CHGeoid 2003, Report 03-33 A (ed. U. Marti et al), Bundesamt für Landestopographie (swisstopo), Wabern, Schweiz

Campbell J (1971). *Eine Erweiterung der Theorie des astronomischen Nivellements bei Einbeziehung von Schweremessungen.* Wissen. Arb. Lehrst. Geod. Phot. u. Kart. TU Hannover Nr. 49

Elmiger A (1969). *Studien über Berechnung von Lotabweichungen aus Massen, Interpolation von Lotabweichungen und Geoidbestimmung in der Schweiz.* Mitt. Inst. Geod. Phot. ETH Zürich Nr. 12

Flury J (2002). *Schwerefeldfunktionale im Gebirge - Modellierungsgenauigkeit, Messpunktdichte und Darstellungsfehler am Beispiel des Testnetzes Estergebirge.* Deutsche Geodätische Kommission C 557

Flury J (2006). *Short wavelength spectral properties of gravity field quantities.* J Geod 79(10-11): 624-640. DOI: 10.1007/s00190-005-0011-y

Flury J, Gerlach C, Hirt C, Schirmer U (2006). *Heights in the Bavarian Alps: Mutual Validation of GPS, Levelling, Gravimetric and Astrogeodetic Quasigeoids.* Proc. Geodetic Reference Frames 2006, submitted

Forsberg R, Tscherning CC (1981). *The Use of Height Data in Gravity Field Approximation by Collocation.* Journal of Geophysical Research 86 No B9: 7843-7854

Galle A (1914). *Das Geoid im Harz.* Königl. Preuß. Geod. Inst. Nr 61. Berlin

GOCE GRAND (2005). *GOCE-Graviationsfeldanalyse Deutschland II . Joint Proposal to BMBF Research Theme 2* (ed. R. Rummel et al.) Institut für Astronomische und Physikalis-

che Geodäsie, TU Munich

Gurtner W (1978). *Das Geoid der Schweiz*. Geodätisch-geophysikalische Arbeiten in der Schweiz, Nr. 32. Schweizerische Geodätische Kommission

Heiskanen WA, Moritz H (1967). *Physical Geodesy*. W.H. Freeman and Company, San Francisco

Heitz S (1968). *Geoidbestimmung durch Interpolation nach kleinsten Quadraten aufgrund gemessener und interpolierter Lotabweichungen*. Deutsche Geodätische Kommission C 124

Helmert FR (1880/1884). *Die mathematischen und physikalischen Theorien der höheren Geodäsie*. Teubner, Leibzig (reprint Minerva, Frankfurt a.M. 1961)

Helmert FR (1901). *Zur Bestimmung kleiner Flächenstücke des Geoids aus Lotabweichungen mit Rücksicht auf Lotkrümmung*. Sitzungsberichte Königl. Preuß. Akad. der Wissenschaften zu Berlin. 2. Mitteilung: 958-975

Hirt C (2004). *Entwicklung und Erprobung eines digitalen Zenitkamerasystems für die hochpräzise Lotabweichungsbestimmung*. Wissenschaftliche Arbeiten der Fachrichtung Geodäsie und Geoinformatik an der Universität Hannover Nr. 253

Hirt C (2006). *Monitoring and Analysis of Anomalous Refraction Using a Digital Zenith Camera System.* Astronomy and Astrophysics 459: 283-290. DOI: 10.1051/0004-6361:20065485

Hirt C, Bürki B (2002). *The Digital Zenith Camera - A New High-Precision and Economic Astrogeodetic Observation System for Real-Time Measurement of Deflections of the Vertical.* Proceed. of the 3rd Meeting of the International Gravity and Geoid Commission of the International Association of Geodesy, Thessaloniki (ed. I. Tziavos): 161-166

Hirt C, Seeber G (2005). *High-Resolution Local Gravity Field Determination at the Sub-Millimeter Level using a Digital Zenith Camera System.* Dynamic Planet, Cairns 2005 (ed. P. Tregoning and C. Rizos), IAG Symposia 130: 316-321

Hirt C, Denker H, Flury J, Lindau A, Seeber G (2006). *Astrogeodetic Validation of Gravimetric Quasigeoid Models in the German Alps - First Results*. Accepted paper presented at 1. Meeting of the International Gravity Field Service, Istanbul

Høg E, Fabricius C, Makarov VV, Urban S, Corbin T, Wycoff G, Bastian U, Schwekendiek P, Wicenec A (2000). *The Tycho-2 Catalogue of the 2.5 Million Brightest Stars*. Astronomy

and Astrophysics 355: L27-L30

Jekeli C (1999). *An analysis of vertical deflections derived from high-degree spherical harmonic models.* J Geod 73(1): 10-22. DOI: 10.1007/s001900050213

Jekeli C, Li X (2006). *INS/GPS Vector Gravimetry Along Roads in Western Montana.* OSU Report 477

Kobold F (1957). *Die astronomischen Nivellemente in der Schweiz.* ZfV 82(4): 97-103

Levallois JJ, Monge H (1978). *Le geoid Européen, version 1978.* Proc. Int. Symp. on the Geoid in Europe and the Mediterranean Area, Ancona, 1978: 153-164

Mader K (1951). *Das Newtonsche Raumpotential prismatischer Körper und seine Ableitungen bis zur dritten Ordnung.* Öst Z Vermess Sonderheft 11

Marti U (1997). *Geoid der Schweiz 1997.* Geodätisch-geophysikalische Arbeiten in der Schweiz Nr. 56. Schweizerische Geodätische Kommission

Meier HK (1956). *Über die Berechnung von Lotabweichungen für Aufpunkte im Hochgebirge.* Deutsche Geodätische Kommission C 16

Molodenski MS, Eremeev VF, Yurkina MI (1962). *Methods for study of the External Gravitational Field and Figure of the Earth.* Transl. from Russian (1960). Israel Program for Scientific Translations Ltd, Jerusalem

Moritz H (1980). *Advanced Physical Geodesy.* Wichmann Karlsruhe

Moritz H (1983). *Local Geoid Determination in Mountain Regions.* OSU Report 352

Nagy D, Papp G, Benedek J (2000). *The Gravitational Potential and its Derivatives for the Prism* J Geod 74(7-8): 552-560. DOI: 10.1007/s001900000116

Nagy D, Papp G, Benedek J (2002). *Erratum: Corrections to "The gravitational potential and its derivatives for the prism"* J Geod 76(8): 475-475. DOI: 10.1007/s00190-002-0264-7

Niethammer T (1932). *Nivellement und Schwere als Mittel zur Berechnung wahrer Meereshöhen.* Astronomisch geodätische Arbeiten in der Schweiz, Nr 20. Schweizerische Geodätische Kommission

Petrović, S. (1996). Determination of the potential of homogeneous polyhedral bodies using line integrals. J Geod 71(1): 44-52. DOI: 10.1007/s001900050074

Tenzer R, Vaníček P, Santos M, Featherstone WE, Kuhn M (2005): *The rigorous determination of orthometric heights.* J Geod 79(1-3): 82-92. DOI: 10.1007/s00190-005-0445-2

Table 1 Statistics of the astrogeodetic measurement campaign 2005 in the Bavarian Alps. A single observation refers to vertical deflection values computed from one pair of digital star images acquired with the DZCS. On average, each single solution relies on 90 reference stars and each station on about 4200 reference stars.

Number of stations	103
Double occupations (in different nights)	38
Number of stations per night	$5-17$
Single observations (total)	6700
Single observations (per station)	48
Processed UCAC stars (total)	589000
Processed UCAC stars (per station)	4180

Torge W (2001). *Geodesy, Third Edition*. W. de Gruyter, Berlin, New York

Tsoulis D (1999). *Analytical and Numerical Methods in Gravity Field Modelling of Ideal and Real Masses*. Deutsche Geodätische Kommission C 510

Tsoulis D (2001). *Terrain correction computations for a densely sampled DTM in the Bavarian Alps*. J Geod 75(5-6): 291-307. DOI: 10.1007/s001900100176

Zacharias N, Zacharias, MI, Urban SE, Høg E (2000). *Comparing Tycho-2 astrometry with UCAC1*. AJ 120: 1148-1152

Zacharias N, Urban SE, Zacharias MI, Wycoff GL, Hall DM, Monet DG, Rafferty TJ (2004). *The Second US Naval Observatory CCD Astrograph Catalog (UCAC2)*. The Astronomical Journal 127: 3043-3059

Table 2 DTM resolution used for the distance zones around each computation point.

zone	outer limit	mesh width	method
1	200 m	10 m / 50 m	cuboids / polyhedra
2	5 km*	50 m	cuboids
3	10 km*	200 m	cuboids
4	80 km	1 km	cuboids
5	150 km	4 km	cuboids
6	350 km	16 km	cuboids

* less for the southernmost part of the profile due to the limited LVG data

Table 3 Near-zone contribution: differences of topographic deflections (in arc seconds) using various methods, DTM resolutions and DTM versions for innermost zone 1

methods / grids		mean	max	min	RMS
50 m cuboids	η	0.001	0.148	-0.124	0.024
- 10 m cuboids	ξ	0.001	0.122	-0.070	0.018
50 m polyhedra	η	0.000	0.176	-0.079	0.019
- 10 m cuboids	ξ	0.000	0.086	-0.081	0.012
new - old DTM,	η	0.006	0.160	-0.070	0.026
50 m polyhedra for both	ξ	0.000	0.082	-0.152	0.019

Table 4 RMS of the $(\Delta\xi, \Delta\eta)$ deflection data computed from the noise vector $\mathbf{n}$

| DTM data set	RMS$_{\Delta\xi}$ [$''$]	RMS$_{\Delta\eta}$ [$''$]
50 m cuboids	0.085	0.082
50 m polyhedra	0.086	0.078
10 m cuboids	0.081	0.079
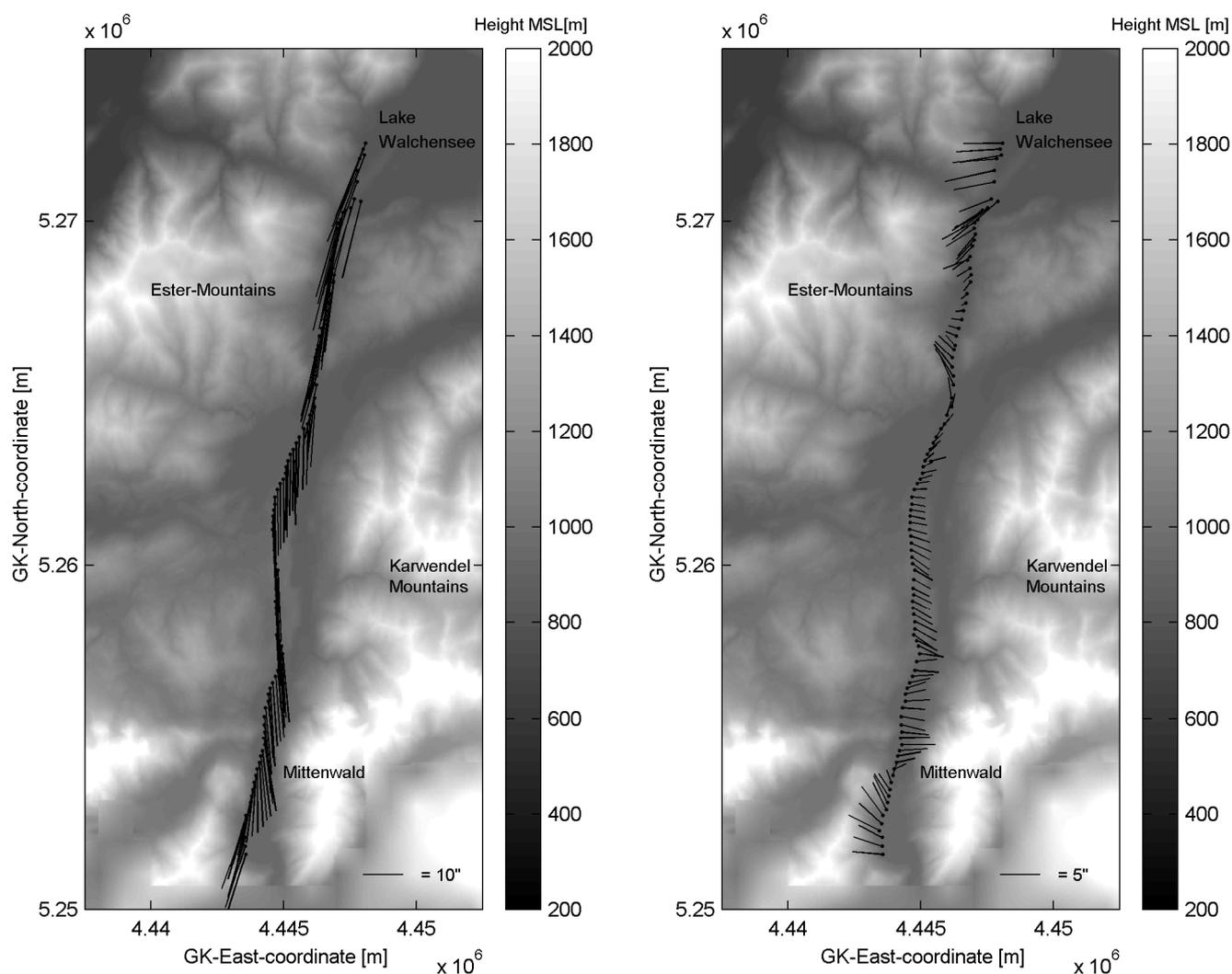
Fig. 1 Vertical deflections, collected with the TZK2-D DZCS in the Bavarian Alps. Located in the Isar valley, the astrogeodetic profile starts at the lake Walchensee and ends near the German-Austrian border. The left panel shows the original vertical deflection data as observed. The set contains a strong trend in southern direction due to the attraction of the Central Alps. Detrending the vertical deflections removes the impact of the Central Alps and makes the gravitational attraction of the local topography clearly visible (right panel). The obtained field of vertical deflections shows the direction variations of the local gravity vector from station to station. GK = Gauss-Krüger coordinate system.

Table 5 Formation of 629 different subsets

name of set	station count	spacing [m]	shift
reference	103	230	0
subset 2_0	51	460	0
subset 2_1	51	460	1
subset 3_0	34	690	0
subset 3_1	34	690	1
subset 3_2	34	690	2
subset 4_0	25	920	0
subset 4_1	25	920	1
subset 4_2	25	920	2
subset 4_3	25	920	3
subset 5_0	21	1150	0
...	...	...	...
subset 35_0	3	8050	0
...	...	...	...
subset 35_34	3	8050	49

Table 6 Statistics for the predicted deflections ξ and η as a function of the spacing between stations with observed deflection data. #stat dep is the number of stations with known deflection data used in the prediction. #stat ind refers to the number of independent stations used for the computation of the statistics.

Description of subset				Component ξ				Component η			
subset no.	spacing [m]	#stat dep	#stat ind	min [″]	max [″]	mean [″]	RMS [″]	min [″]	max [″]	mean [″]	RMS [″]
2_0	460	51	51	−0.25	0.30	0.00	0.11	−0.39	0.27	−0.01	0.12
3_0	690	34	68	−0.36	0.34	−0.02	0.17	−0.29	0.24	−0.00	0.15
4_0	920	25	75	−0.28	0.34	0.02	0.19	−0.43	0.31	0.02	0.21
5_0	1150	20	80	−0.32	0.31	−0.06	0.26	−0.24	0.30	0.16	0.25
6_0	1380	17	85	−0.32	0.30	−0.06	0.26	−0.42	0.25	0.03	0.27
8_0	1840	12	84	−0.32	0.30	−0.02	0.35	−0.36	0.35	0.23	0.35
10_0	2300	10	90	−0.51	0.33	−0.36	0.47	−0.39	0.35	0.04	0.38
17_0	3910	6	96	−0.74	0.58	−1.28	1.15	−0.37	0.41	0.45	0.69
26_0	5980	3	75	−0.88	1.01	4.95	2.67	−0.54	0.27	−3.12	1.13
35_0	8050	2	68	−0.77	0.57	−1.49	2.00	−0.57	0.27	−3.62	1.33

Table 7 Statistics of the comparison between the two independent subsets 2_0 and 2_1

spacing [m]	min [mm]	max [mm]	mean [mm]	RMS [mm]	std. dev. [mm]
460	−1.50	0.11	−0.82	0.91	0.6

Table 8 Comparison between LSC (use of the 50 m DTM data) and linear interpolation (without DTM data). The spacing between observed vertical deflection stations ranges from 230 m to 2300 m. The RMS is accumulated over the complete profile length of 23 km. The maximum differences refer to the total profile length.

Levelling approach:	astron.-topograph.		astronomical	
Interpolation technique:	LSC		linear	
Use of DTM data:	yes		no	
spacing	max diff	RMS	max diff	RMS
[m]	[mm]	[mm]	[mm]	[mm]
230	0.00	0.00	1.26	1.01
460	0.78	0.44	21.99	3.58
690	0.83	0.34	24.65	3.52
920	0.76	0.26	30.12	17.96
1150	0.93	0.42	39.89	24.06
1380	1.18	0.45	22.31	6.54
1610	4.28	2.68	39.21	22.58
1840	2.81	0.68	22.13	13.11
2070	2.46	1.22	78.44	45.98
2300	3.73	1.46	96.47	56.16

Table 9 Accuracy of astronomical-topographic levelling as a function of the station spacing. spa = spacing of the stations and len = length of the profile. The table shows the attainable accuracy in [mm] for a quasigeoid height difference over some profile lengths given in the first column. The station spacing is listed in the first row. Note that the impact of systematic errors is not included.

spa. [km]	0.5	0.75	1	2	3	4	5	6
len. [km]								
10	0.4	0.6	0.8	1.6	4.1	6.4	8.0	11.0
20	0.6	0.8	1.1	2.3	5.8	9.1	11.3	15.6
30	0.7	1.0	1.4	2.8	7.1	11.1	13.9	19.1
40	0.8	1.2	1.6	3.2	8.2	12.8	16.0	22.0
50	0.9	1.3	1.8	3.6	9.2	14.3	17.9	24.6
75	1.1	1.6	2.2	4.4	11.2	17.5	21.9	30.1
100	1.3	1.9	2.5	5.1	13.0	20.2	25.3	34.8
200	1.8	2.7	3.6	7.2	18.3	28.6	35.8	49.2
300	2.2	3.3	4.4	8.8	22.5	35.1	43.8	60.2
400	2.5	3.8	5.1	10.1	25.9	40.5	50.6	69.6
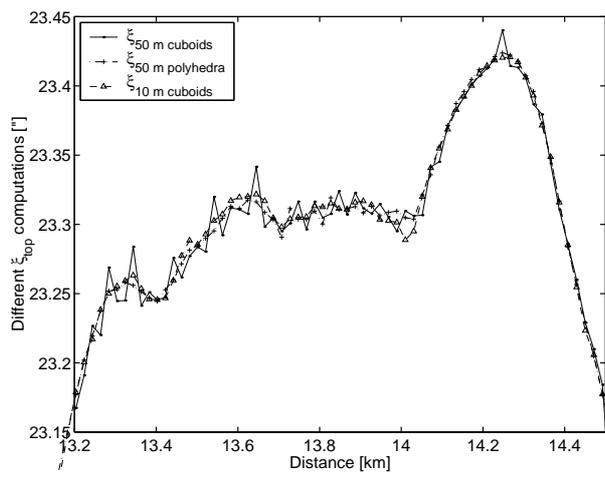
Fig. 2 Topographic deflection component ξ computed from different DTM data and geometric bodies in the innermost zone 1. Note that the topographic deflections computed from 50 m polyhedra and 10 m cuboids coincide well and show a smoother behaviour than those derived from 50 m cuboids.
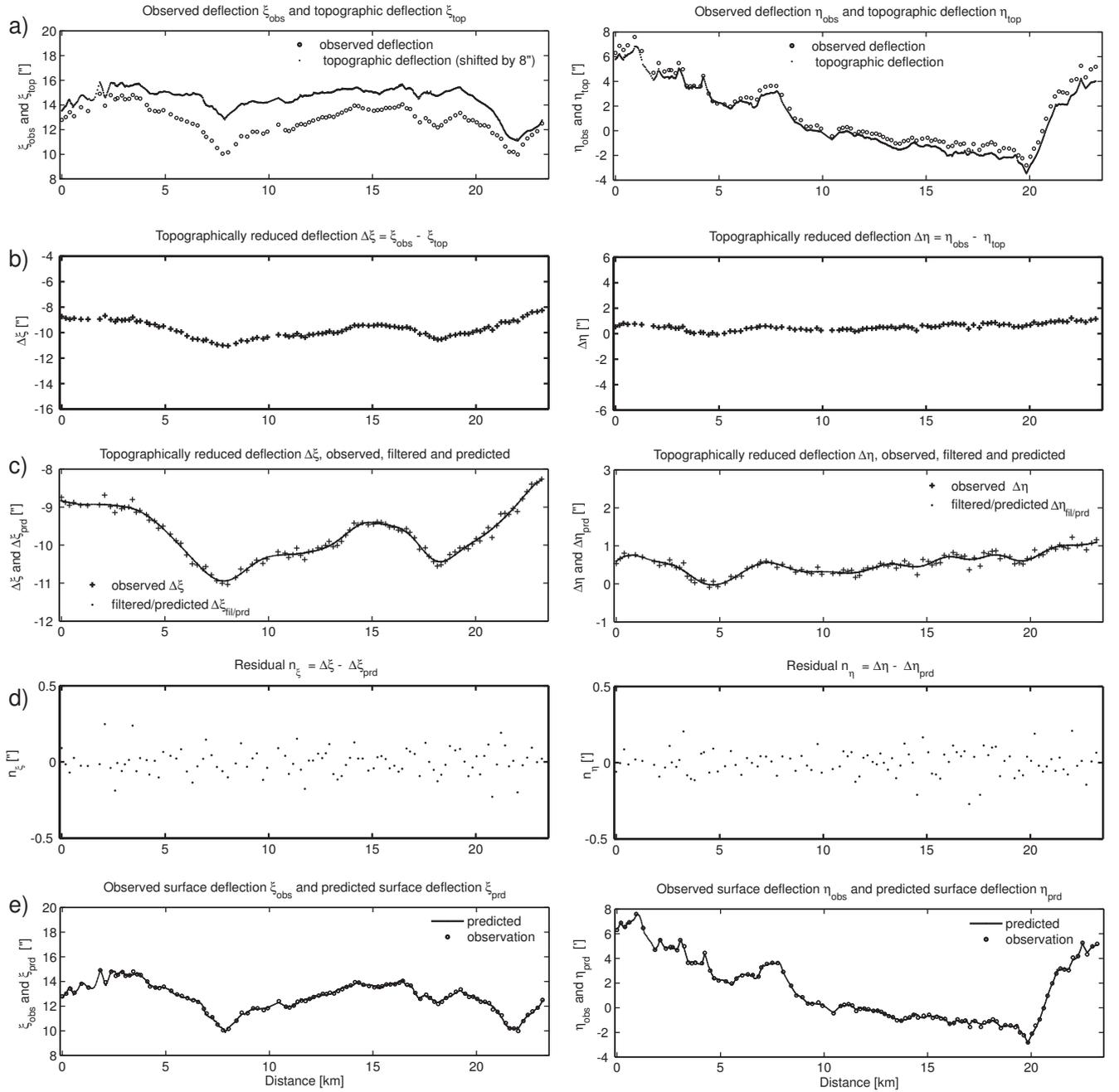
Fig. 3 Combination approach for the interpolation. The left column shows the results for ξ and the right column for η, both as a function of the profile distance. (a): observed and topographic deflections. (b): topographically reduced deflections, on the same scale as used in (a). (c): topographically reduced deflections, on a larger vertical scale. Filtered and predicted reduced vertical deflections are shown. (d): residual noise vector **n**, showing the differences between topographically reduced and filtered deflections. (e): dense data sets of predicted surface deflections shown together with the astrogeodetic observations. Note that the striking peak-like structures, especially apparent in (a) and (e) as well as partly in (c), originate from azimuth changes between adjacent profile sections (cf. Fig. 1).
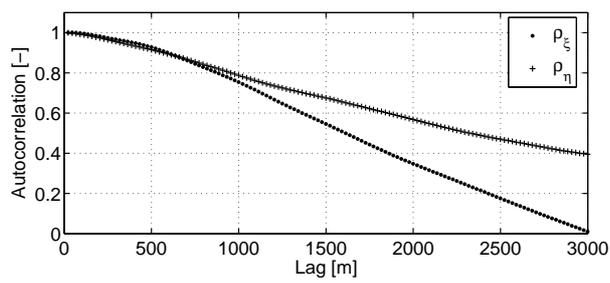
Fig. 4 Autocorrelation ρ of $\Delta\xi$ and $\Delta\eta$ as function of the lag
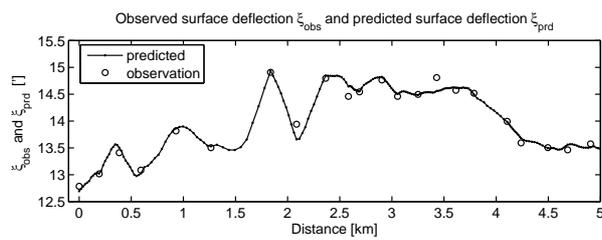
Fig. 5 Predicted surface vertical deflection ξ_{prd} in the profile range $0 - 5$ km. Note that the peaks, e.g., at 0.3 km, 1.7 km and 2.1 km, originate from azimuthal changes of the profile (cf. Fig. 1, station arrangement at Lake Walchensee).
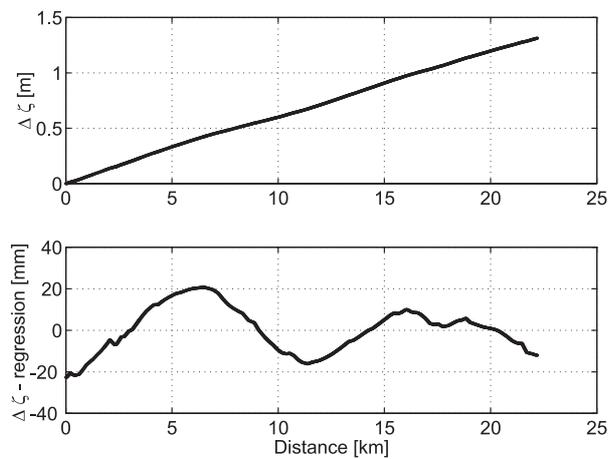

Fig. 6 Top: Astrogeodetic quasigeoid profile in the Bavarian Alps, computed from 103 astrogeodetic observations and DTM data. Bottom: Detrended profile (difference between the quasigeoid profile and a regression line) reveals the fine structure
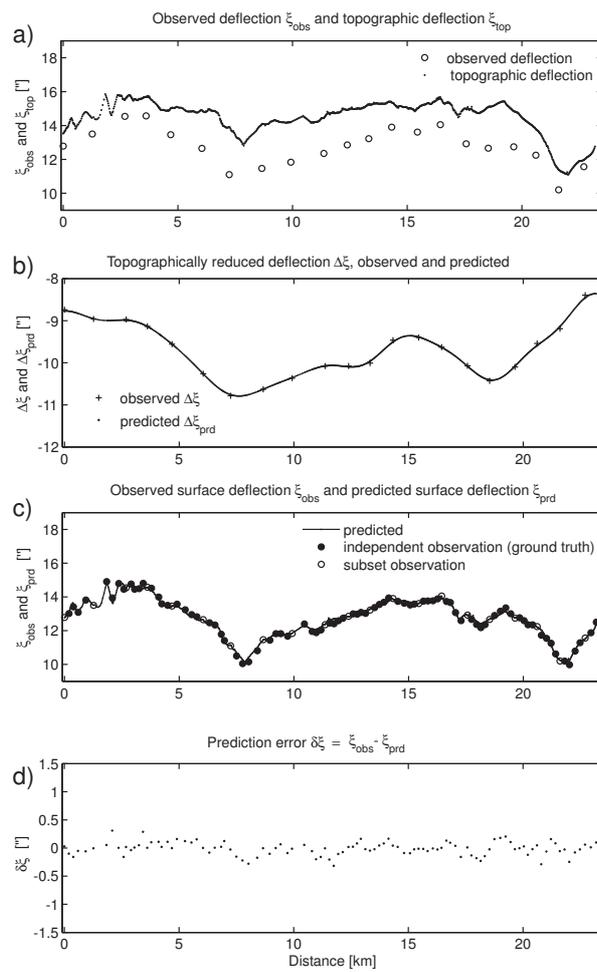
Fig. 7 Use of a vertical deflection $(\xi, \eta)_{obs}$ subset for prediction of $(\xi, \eta)_{prd}$ data. (a): observed and topographic deflections. (b): topographically reduced deflections. (c): predicted surface deflections shown together with the astrogeodetic observations used in the prediction (open circle) and independent observations (full circle) (d): Prediction error $\delta\xi$, computed with respect to the independent observations.
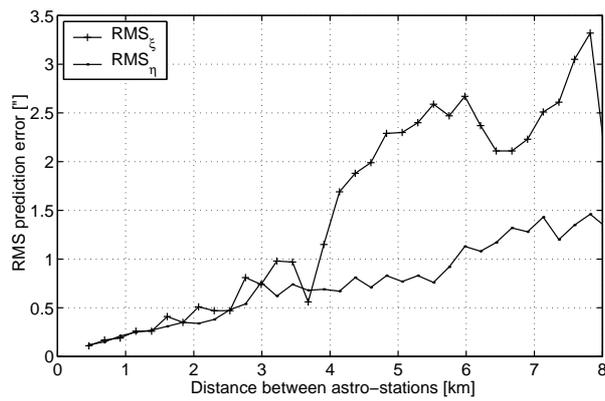
Fig. 8 RMS prediction error for surface vertical deflections $(\xi, \eta)_{prd}$ as a function of the station spacing
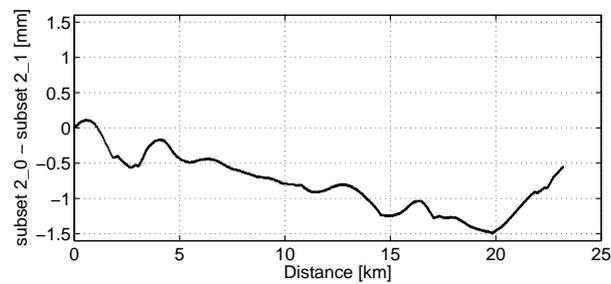
**Fig. 9** Differences of the two independent astrogeodetic profiles computed from subsets 2_0 and 2_1
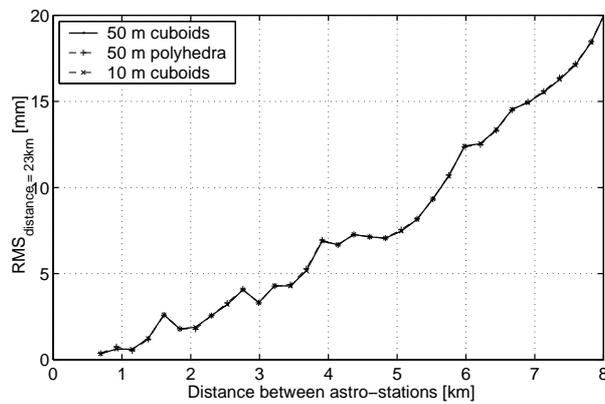
**Fig. 10** RMS for different DTM data and computation methods
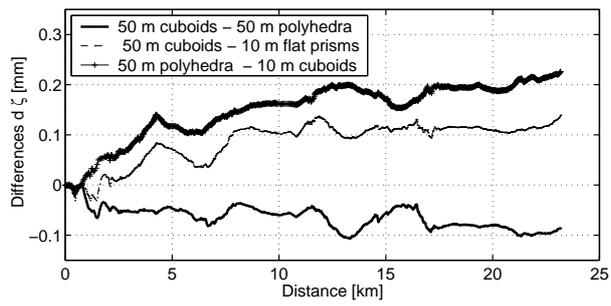
Fig. 11 Quasigeoid differences computed from 103 astrogeodetic vertical deflections and three different DTM data sets
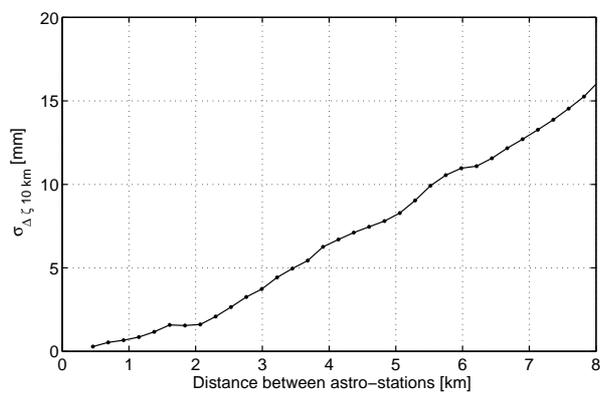

Fig. 12 Standard deviation σ for the quasigeoid height difference over a profile length of 10 km as a function of the station spacing